Performance and capacity of composite "mega columns" with encased hot rolled steel sections

Teodora Bogdan*[,a], Jean–Claude Gerardy[b], Donald W. Davies[c], Nicoleta Popa[a]

[a]ArcelorMittal Global R&D,Structural Engineering Department, Luxembourg
teodora.bogdan@arcelormittal.com, nicoleta.popa@arcelormittal.com
[b] ArcelorMittal Europe – Long Products, Luxembourg
jc.gerardy@arcelormittal.com
[c] Magnusson Klemencic Associates, USA
ddavies@mka.com

ABSTRACT

Steel reinforced concrete (SRC) columns are widely used in high-rise buildings, since they provide larger bearing capacity and better ductility than traditional reinforced concrete (RC) columns. This type of structural system is not currently explicitly addressed in the actual design codes.
The paper aims at presenting the behaviour of a new configuration of mega columns - isolated steel reinforced concrete (ISRC) columns. A two-phase test was conducted on scaled ISRC columns designed based on a typical mega column of a super high-rise building. Phase 1 of the study includes six 1/4-scaled ISRC columns under static loads: every two of the specimens are loaded statically with the eccentricity ratio of 0, 10%, and 15%, respectively. Phase 2 of the study includes four 1/6-scaled ISRC columns under quasi-static loads: every two of the specimens were loaded under simulated seismic loads with the equivalent eccentricity ratios of 10% and 15%, respectively. A finite element analysis (FEA) was conducted as a supplement to the physical tests to provide a deeper insight into the behaviour of "mega columns". An extended Plastic Distribution Method is defined to evaluate the capacity of the specimens. The method is based on simplifications similar to those proposed in EC4 [1]. The scope of this latter standard is limited to the consideration of one single steel profile. The method is validated by comparisons with experimental and with numerical simulation results using advanced finite element programs, showing a good accuracy in results.

Keywords: steel concrete composite mega column, separate steel sections, down-scaled experimental tests, Plastic Strain Distribution Method

1 INTRODUCTION

1.1 Research background and overview

There is an ongoing need to optimize construction materials and reduce the size of elements required within the structural systems of high-rise buildings. Minimizing the size of the vertical structural elements, without compromising the economic feasibility of projects and limiting their significant share on tall buildings' floor plans, is a consistent challenge. The use of composite structural elements, such as combining concrete and steel, along with higher grade materials within each, is a viable solution.
Currently, concrete filled tubes (CFT) or concrete filled continuous caissons built-up by welding heavy plates are the common structural solutions. Their main drawbacks include high costs, the need for skilled labour, complex connections, and requiring welding conditions for heavy plates, such as preheating and repairing.
Composite mega columns considered in this research are defined as vertical structural systems with several hot-rolled steel sections embedded in concrete, and subjected to significant vertical loads and bending moments from seismic actions.

Although codes and specifications do consider composite structural elements, they do not offer specific provisions on the design of composite sections with two or more encased steel sections (AISC 2016 Specifications for instance).
The lack of knowledge on the axial, bending and shear behaviour of composite mega columns, along with the resulting lack of clarity in the codes, leads to the need for experimental performance tests. These tests provide a simplified design approach and help develop numerical methods to describe the designs and to validate the results. The experimental campaign took place within CABR Laboratories and the Laboratories of Tsinghua University, Beijing.
The results of the experimental campaign are used to investigate the specimens' maximum capacity, displacements, stress distribution, ductility and stiffness.
Experimental results are validated by finite element method (FEM) models with the numerical values in accordance with the experimental values. FEM models allow also for a deeper insight on steel-concrete interaction forces and stress distribution.
Finally, simplified design methods based on European, Chinese, and US codes are suggested and the results are compared to the numerical and experimental values. Then, through three examples of application to selected mega column sections, the simplified methods are proven to be an effective and handy design tool.

2 EXPERIMENTAL CAMPAIGN

The column specimens' overall layout and geometry have been based on suggested sections of representative full scale composite columns used for high-rise buildings, from Magnusson Klemencic Associates, Seattle (MKA). Overall dimensions of the columns are 1800 x 1800 mm, with a height of 9 m at the lobby level (base of the tower) and 4.5 m at the typical floor. The experimental campaign is divided in 2 phases: 6 static tests and 4 quasi-static tests.

2.1 Phase 1 - Static tests

Phase 1 contains 6 specimens with the same geometry configuration, detailed in *Fig. 1*. The specimens are tested to failure by applying concentrated load, using a 200-tons servo system at Tsinghua University [2]. The experimental setup consists in two hinges, as shown in *Fig. 2*. One hinge is placed on the ground and fixed by blocks to avoid any horizontal displacements. The other one is placed on the top of the test specimen, connected to a transition beam that serves as a connector between the hinge, horizontal actuator and the vertical actuator.
Sand layers are placed between the test specimens and the hinge, and polytetrafluorethylene plates are placed under the end plates of the steel sections, to make sure that the steel – concrete interface slip can be developed near the test specimen ends to simulate real boundary conditions. In real structures, relative slip may occur along the composite column at any point. If the sand layers and PTFE plates are not provided, the rigid surface of the hinge will force the test specimen end to stay in the same plane. Consequently, relative displacement between the concrete and the steel sections near the test specimen ends will be limited, which overestimates the composite column.

Table 1. Obtained material strengths (Units: MPa)

Specimen ID	Actual eccentricities e/h [%]	Concrete cubic strength	Yield strength of steel section flange	Yield strength of steel section web	Yield strength of longitudinal bar	Yield strength of transverse bar
E00 – 1	0.0	61.17	408	523	438	$f_{3.25}$ = 597 $f_{4.80}$ = 438
E00 - 2	0.0	56.62	398	411		
E10 – 1	12.4	59.75	423	435		
E10 - 2	12.9	68.40	383	415		
E15 – 1	19.9	67.50	377	404		
E15 - 2	17.9	75.17	389	405		

The loading rate is slow enough to avoid dynamic effects. Loads are increased to peak value until the specimens failed. Each two of specimens were loaded under same eccentricity ratio e/h: 0%, 10% and 15%. Due to second order effects, the actual eccentricity ratios got larger. The exact values of these eccentricities are presented in *Table 1*. During the test, the lateral displacement of the transition beam is strictly controlled by the horizontal actuators to ensure lateral displacement of the top end has zero value.

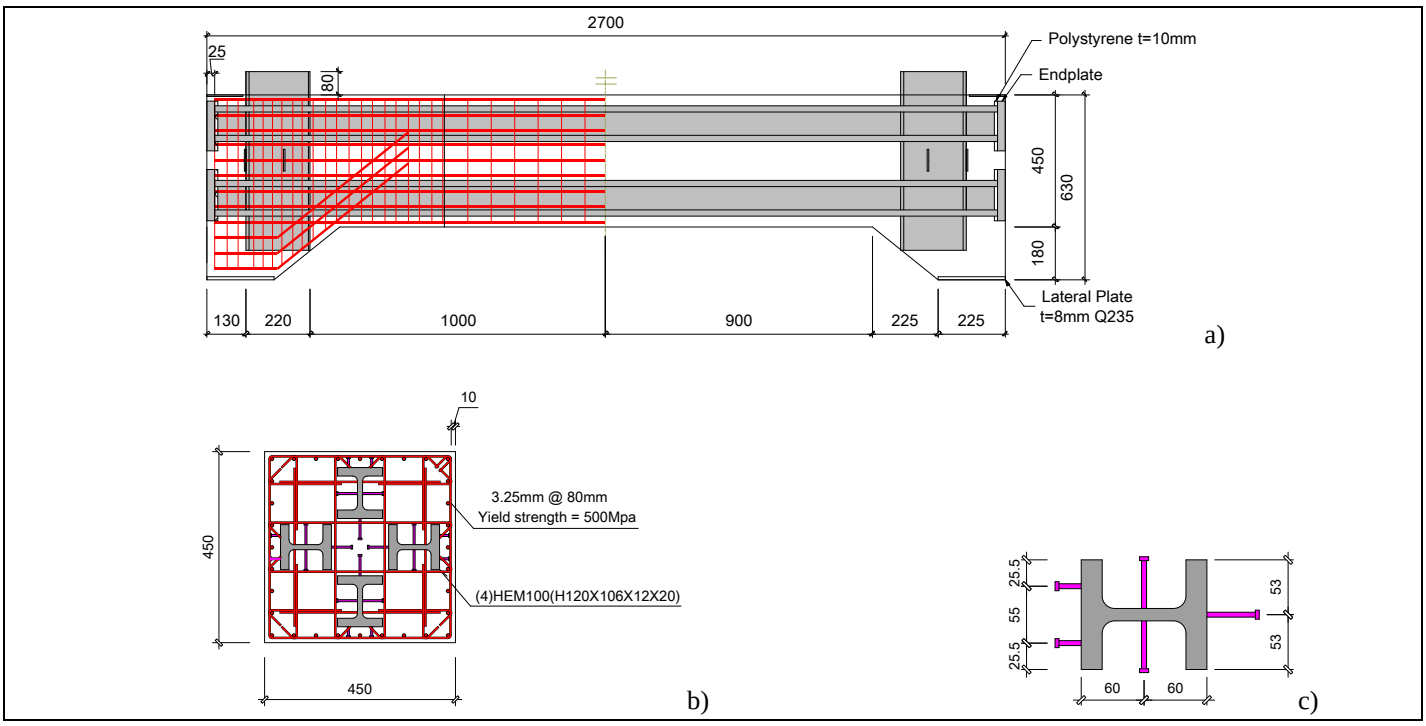

Fig.1. Details of the static tests: a) steel layout – longitudinal view; b) Cross section details; c) Shear studs layout.

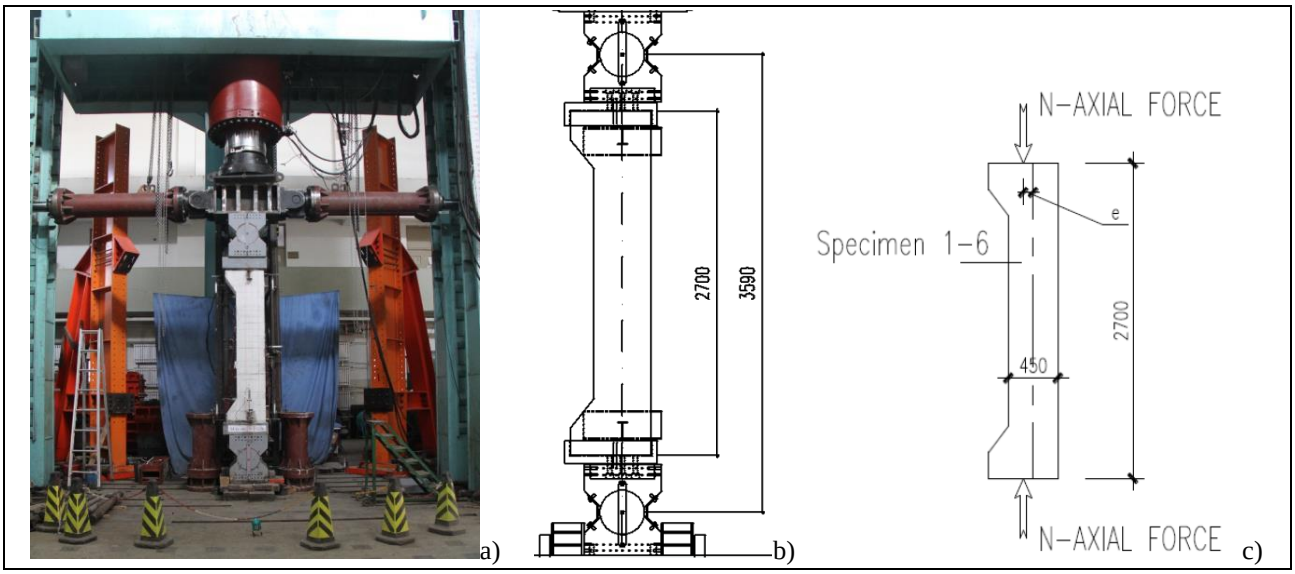

Fig.2. Phase 1: Test setup: a) static setup in laboratory b) boundary conditions; c) load application.

The data in this test program include measuring the strain on the profiles, longitudinal bars, ties and concrete surface. The strain sensors are placed on four sections for each specimen, as shown in *Fig. 3*. The displacement sensor consists in two parts: a slide rheostat and a steel box. The slide rheostat is stuck on the surface of the steel section, surrounded by the steel box and the steel box is

surrounded by concrete. During the test, the slide rheostat will move with the steel section and the box will move with the concrete, so the relative displacement can be detected.

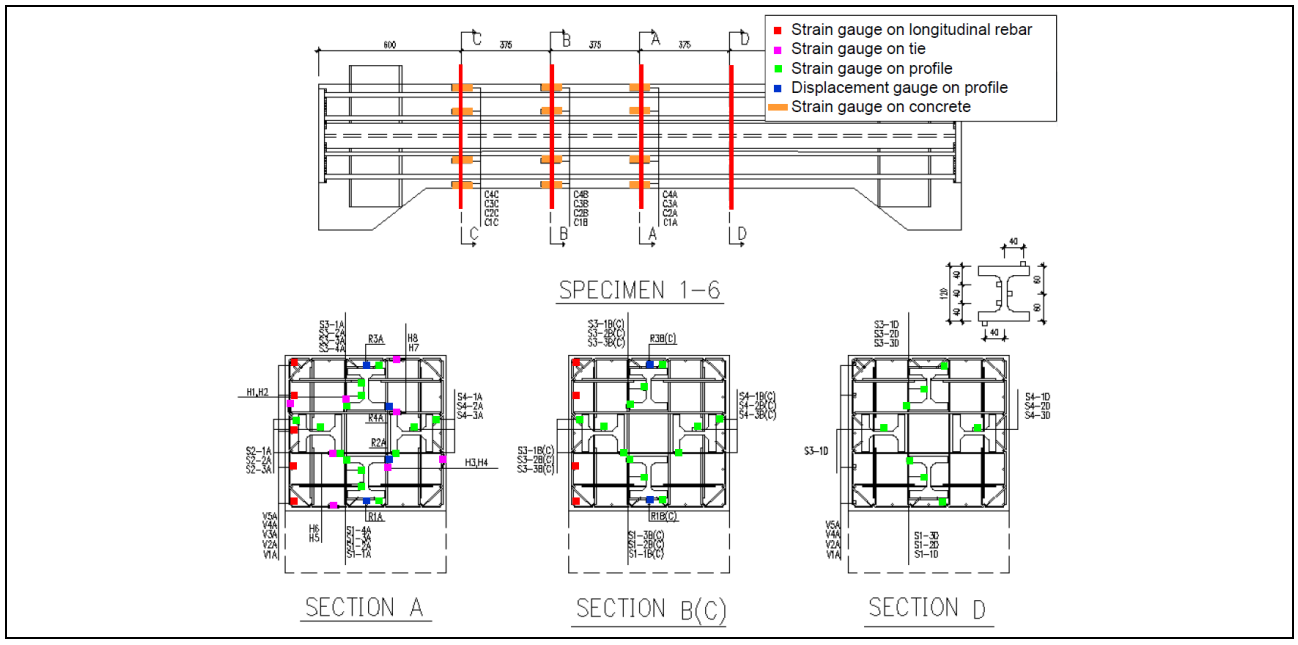

Fig.3. Phase 1: Configuration of strain and displacement gauges.

The static test results confirm the composite mega column expected behaviour, and provide additional evidence of vertical and lateral displacements, curvature and ductility, axial and bending stiffness, and relative displacements between steel sections and concrete.

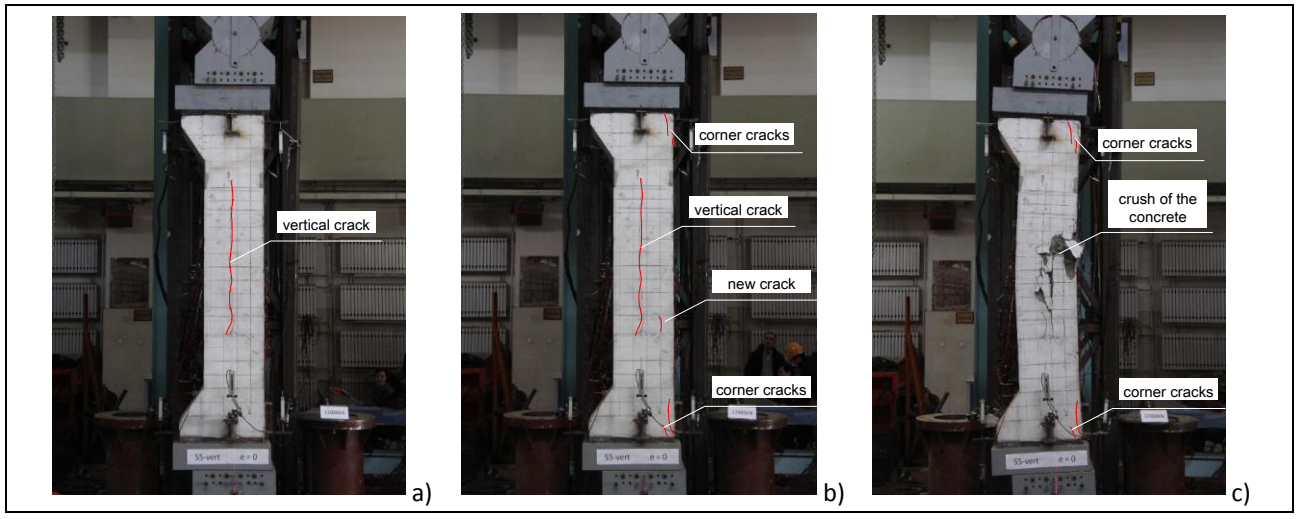

Fig.4. Crack development of specimens subjected to axial load: a) 70% of the maximum load; b) after the maximum load; c) failure load.

As the axial load increases, cracks develop – at first vertically, where the concrete cover is limited, and then horizontally, when the specimen is reaching failure. When the deflections are large, the axial load decreases in value and the test stops. On purely axial specimens, the axial load start decreasing after reaching the peak value due to an increased vertical deflection. The second load drop occurs when the column fails, when sudden, significant deflections and damage occurs. Eccentric specimens do not experience a sudden drop of applied load, as the axial load gradually decreases after the peak point. Meanwhile, the horizontal deflection and concrete damage continuously develop, especially on areas of the concrete under tension. On purely axial specimens, buckling of the longitudinal rebar and breakage of ties are observed.

Fig. 4 and *Fig. 5* present the crack development during the loading phase. Steel profiles yield, but do not buckle. No significant deformations of the profiles are registered.

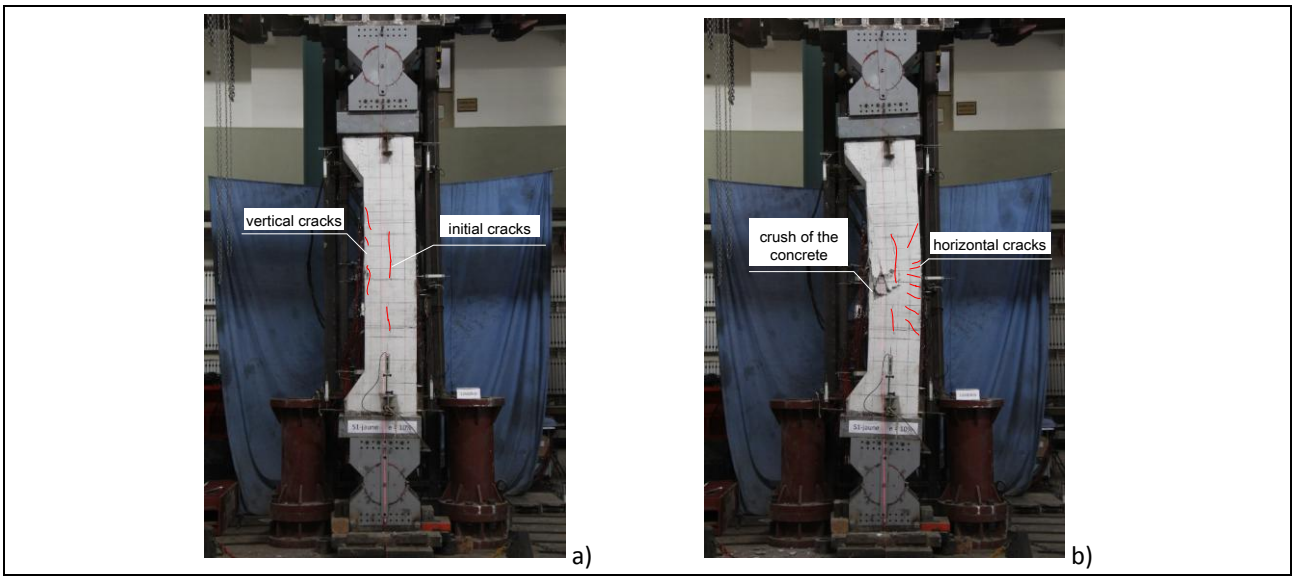

Fig.5. Crack development of specimens subjected to eccentric loads: a) 70% of the maximum load; b) failure load.

Fig. 6a presents the bending moment vs. rotation at the mid section of the specimens. It can be observed that the bending moment of the mid section remains constant at the curvature develops. The slopes of the curves become smaller with the increase of rotation, suggesting that the bending stiffness decreases as the load increases. Knowing the dimension of the moment, multiplied by the angle is energy, it means the area under the 'moment vs. rotation' curve is a reflection of absorbed energy of the mid-section. Thus, the ductility of the column in terms of 'moment vs. rotation' is excellent for columns with an eccentricity ratio less than 15%.

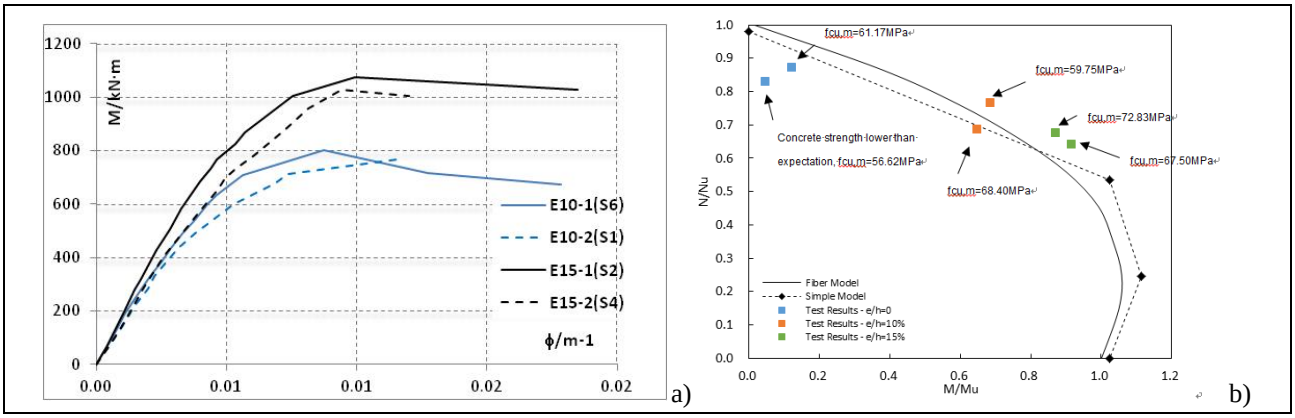

Fig. 6. a) Moment vs. rotation at mid-section; b) bending moment – axial force interaction curves

In *Fig 6b* the experimental interaction points correspond with the simplified interaction curve (according to Plumier method, et al.) [3], [4]. Interaction curves are calculated using the average material strengths of the test specimens, resulting in divergences between the curves and recorded data points. The design value of axial load is not reached because the concrete is crushing outside the confined zone and the concrete crushing strains outside the stirrups is below the design value of 3.5-E-3. For specimens subjected to eccentric loads, test results show good convergence with the curves. For specimens subjected to axial loads, test results are smaller than predictions given by both the fiber model and the simplified method. Reasons for that include: (1) concrete strengths of these two specimens are lower than the average value of the six, and (2) the calculated results have not considered buckling effects and P-Δ effects yet.

As no shear force occurs, it can be assumed that the strain of the steel profiles, concrete, and longitudinal rebar is identical in each section. Longitudinal rebars and steel sections remain elastic when the purely axial specimen reaches the maximum capacity. On eccentric specimens, longitudinal rebars and steel sections yield before the specimen reaches the maximum capacity. The strain distribution of the mid section validates the 'Plane Section Assumption' in this phase of the test.

EC4 defines the stiffness of a column having one embedded steel profile using *Eq. (1)*. The experimental value of the effective flexural stiffness can be determined using the curvature definition of the beam theory. The Euler- Bernoulli beam theory defines the curvature with *Eq. (2)*.

$$(EI)_{eff} = E_a \cdot I_a + E_s \cdot I_s + K_e \cdot E_{c,eff} \cdot I_c \quad (1)$$

$$\chi = \frac{1}{\rho} = \frac{M}{(EI)} \quad (2)$$

where: $K_e = 0.6$ the correction factor

I_a and I_c and I_s are the second moment of area of the structural steel section, the un-cracked concrete section and the reinforcement

E_a and E_c and E_s are the second moment of area of the structural steel section, the un-cracked concrete section and the reinforcement

χ - the curvature and ρ - the radius of curvature.

The reduction factor for flexural rigidity can be defined using the following approach:

$$M = (E_a \cdot I_a + E_s \cdot I_s + R_b^k \cdot E_{cm} \cdot I_c) \cdot \chi \quad (3)$$

The experimental value of the stiffness reduction factor is determined using *Eq. (4)*. *Table 2* presents a comparison between the experimental values and theoretical one. It can be observed a good accuracy of the current design codes, except E10_1 specimen. In conclusion, the evaluation of composite columns with several embedded steel profile can be conducted using available design codes, for columns having an applied axial eccentricity lower than 15%.

$$R_{b\_EC4}^{k} = \frac{(EI)_{eff\_experimentaly} - E_a \cdot I_a - E_s \cdot I_s}{E_{cm} \cdot I_c} \quad (4)$$

Table 2. Stiffness reduction factors – comparisons.

	EC 4 - k_e value	R_{bk_EC4}- Experimental value	Ratio
E10_ 1	0.6	0.462	130%
E10_ 2	0.6	0.599	100%
E15_ 1	0.6	0.612	98%
E15_ 2	0.6	0.599	100%

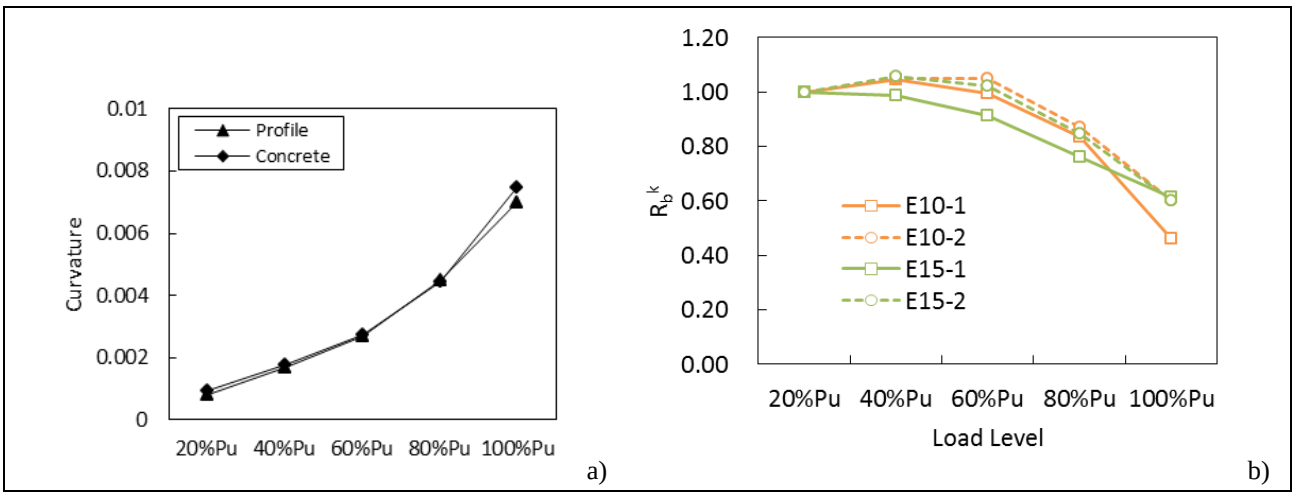

Fig. 7. a) Specimens E10-1 and E10-2 – curvature development; b) flexural rigidity degradation using EC4 design method.

2.2 Phase 2- Quasi -static tests

Phase 2 of the experimental campaign consist in four 1:6 scaled specimens with their geometrical configurations presented in *Fig. 8* and *Table 3.* The behaviour, including the capacity, deformation capacity, and hysteretic performance of the specimens under simulated seismic loads, are examined according to different eccentricities.

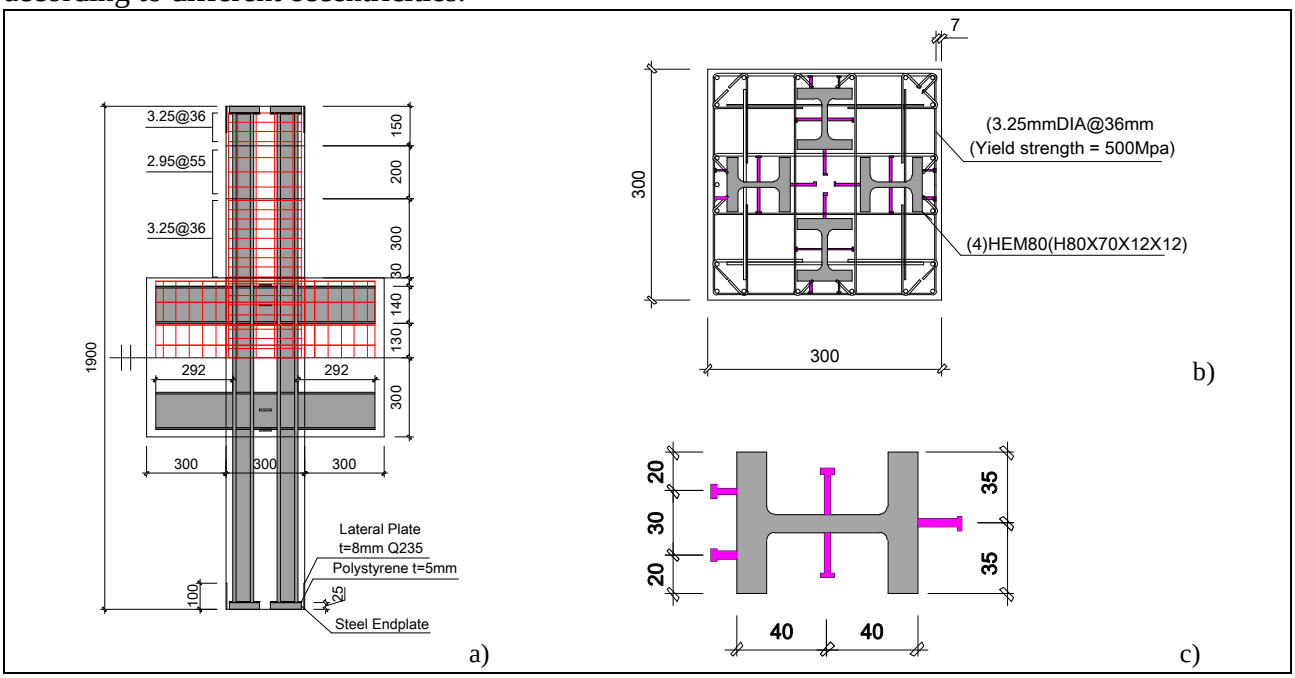

Fig.8. Phase 2: Quasi-static tests: a) steel layout – longitudinal; b) steel layout – cross section; c) shear studs layout.

Table 3. Quasi- static selected materials

Concrete	C60 (fck = 38.5 MPa), with 5 mm aggregate maximum size
Hot rolled jumbo sections	Horizontal: 140x73x4.7x6.9 mm Vertical: HEM80 (80x60x12x12 mm) S235 (fyk = 235 MPa = 34 ksi)
Longitudinal reinforcement	6 / 8 mm dia - HRB400 (ASTM A615), (fyk = 400 MPa)
Stirrups	3.25mm dia @ 36 mm HRB500 (fyk = 500 MPa)
Shear studs	5mm DIA x 25 mm Nelson headed Studs; ASTM A108 @ 150 mm O.C. 5mm DIA x 15 mm Nelson headed Studs; ASTM A108 @ 150 mm O.C Grade 4.8

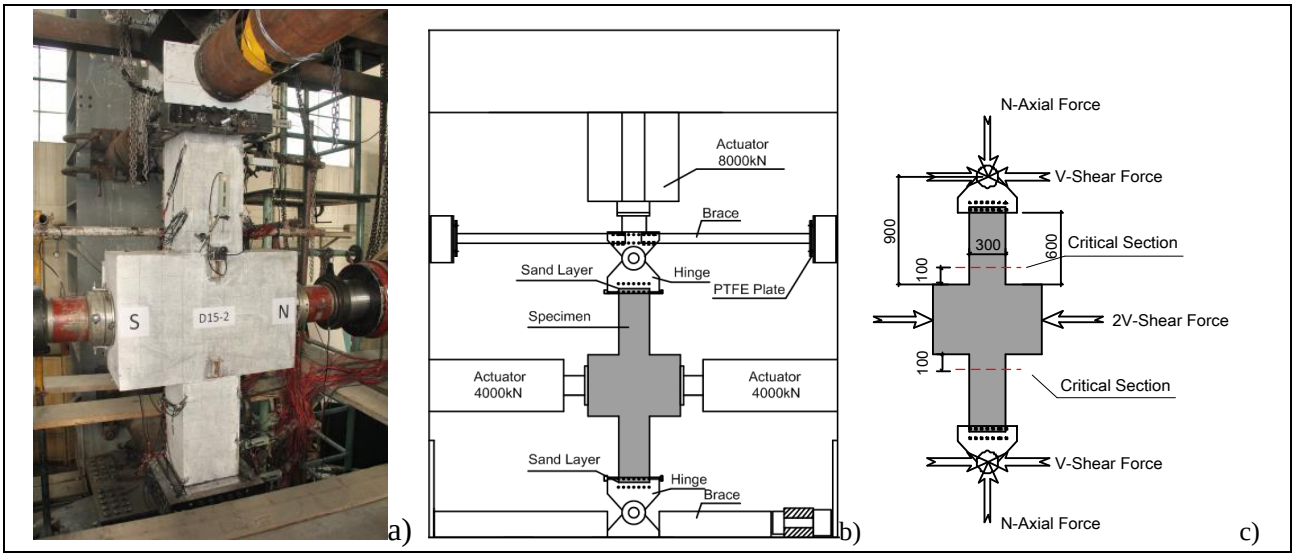

Fig.9. Phase 2: Quasi-static tests: a) laboratory setup; b) boundary conditions; c) test setup.

Axial force with different eccentricities values: 10% - specimens D10-1 and D10-2, and 15% - specimens D15-1 and D15-2, to account for the diversity in materials and fabrication. Horizontal force is applied at the mid-height of the specimens. Transverse load (V) is equal to two times the horizontal end reaction on the top and bottom of the specimens. A bottom hinge is placed on the ground and a top hinge is installed on the top of the specimen, connecting it to the vertical actuator. Both the hinges are fixed by a frame that restricts horizontal displacements, as well as out-of-plane displacements (*Fig. 9c*).
As shown in *Fig. 10*, axial load slowly increases until it reaches the gravity load. Then, the axial load and the transverse load are increased proportionally. The axial load is increased by 500 kN steps, and the lateral load is applied cyclically, while keeping the axial load constant.

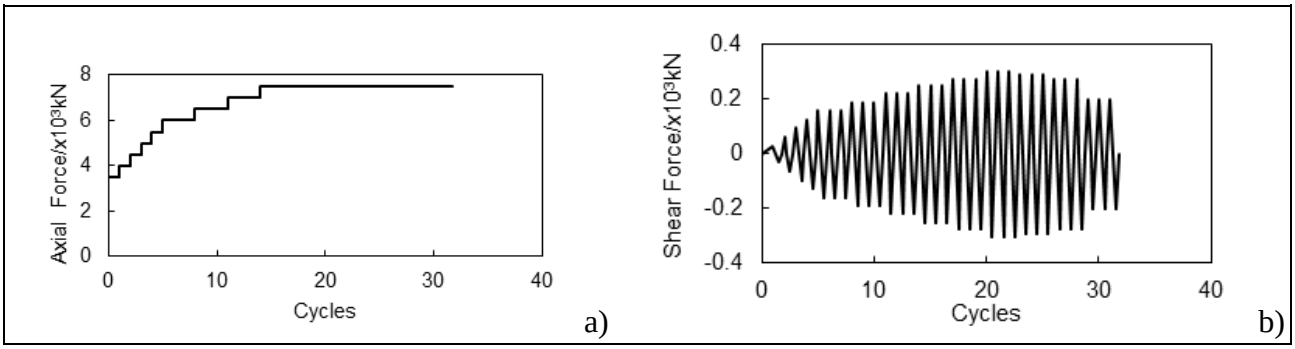

Fig. 10. Phase 2: Load introduction: a) axial load history; b) horizontal load history.

General behaviours of the quasi-static tests are quite alike because the eccentricity ratios do not differ much. Crack distributions and failure modes indicate that the specimens fail in combined compression and flexure patterns, as shown in *Fig. 11*. When the first step of the loading is completed, the test specimens do not show significant deformations and cracks. During the second step of the loading, cracks and concrete crush gradually develop, and the cumulative damage at the column corners leads to the failure of the specimen.

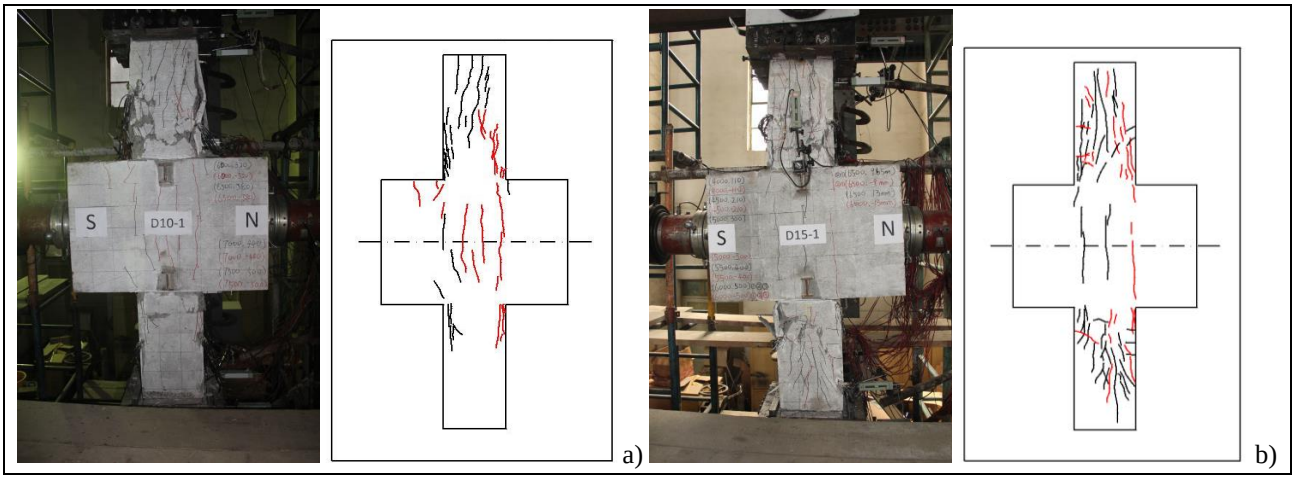

Fig. 11. Phase 2: Crack distribution and failure modes of specimens: a) Specimen D10-1; b) Specimen D15-1.

The hypothesis on the static tests, known as the 'Plane Section Assumption,' is verified within the 15% eccentricity ratio. Despite the damage to the concrete cover, the core concrete remains intact due to the confinement effect provided by the steel sections. The concrete core confinement prevents the steel sections from buckling. Local buckling of longitudinal rebar and breakage of the transverse ties are detected. The ability to dissipate energy is shown by stable and round hysteretic curves, without a large dependence on the eccentricity ratio (*Fig. 12*).

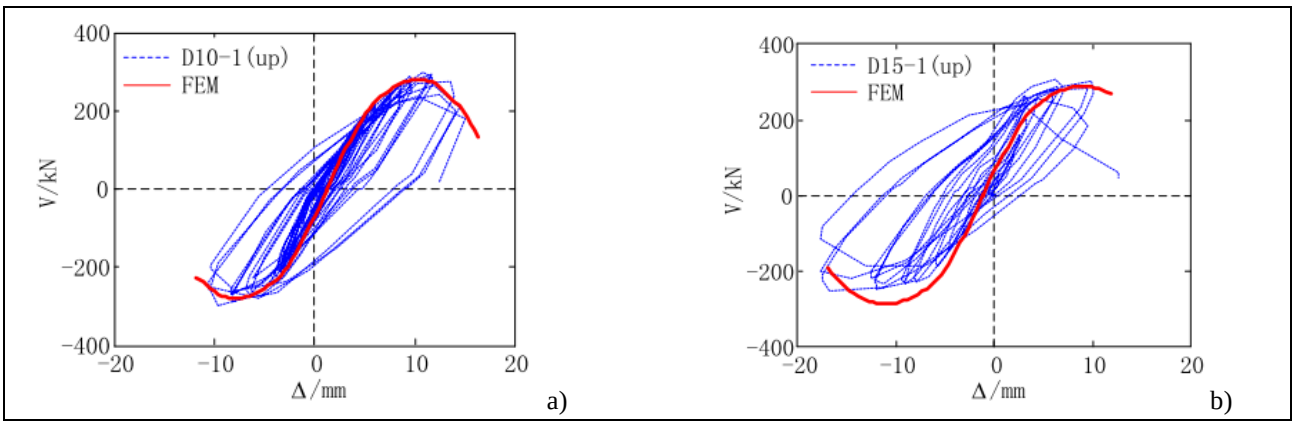

Fig.12. Phase 2: hysteretic curves a) Specimen D10-1; b) Specimen D15-1.

For specimens tested with 10% eccentricity until failure, strain distribution of concrete and steel section is linear, so the 'Plane Section Assumption' can be verified. For specimens tested with 15% eccentricity, the assumption is valid under gravity and yield load level. Longitudinal rebar violate the assumption because buckling occurs. Therefore, the plane section assumption is more likely verified within a 15% eccentricity ratio.

3 VALIDATION OF TEST RESULT WITH FEM

FEM analysis has been completed for static tests, using the software Abaqus. For concrete a damaged plasticity model with a confinement effect is adopted. A tri-linear behaviour, with values from the test, is assumed for steel sections and rebar. The concrete and steel sections are simulated by three dimensional eight-node solid elements, and the bars are simulated by two dimensional three-node truss elements. To simplify the model, bars and steel beams are connected with ties to the concrete, so there is no relative displacement or strain difference. The interactions of concrete and steel sections are simulated by nonlinear springs along each dimension as shown in *Fig 13*.

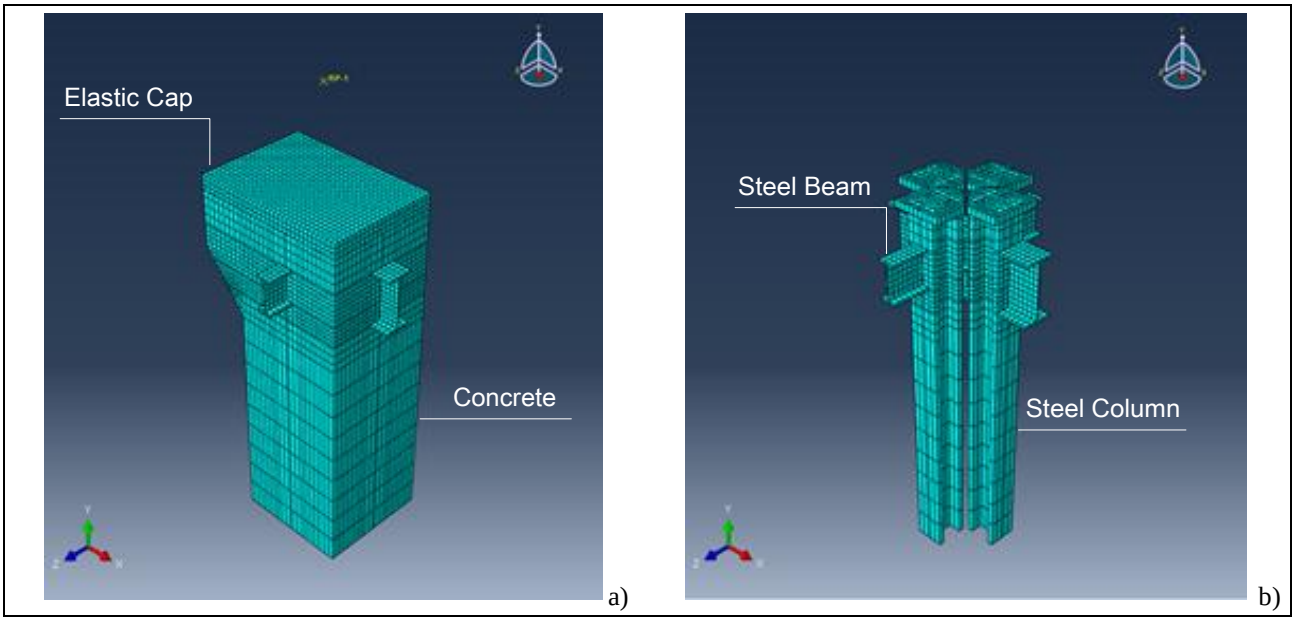

Fig.13. Phase 1: Abaqus FE models: a) concrete mesh; b) steel section mesh.

Before peak point, the calculated 'axial load vs. vertical displacement' curve follows similar paths to the experimental curve. The difference between the curves widen after peak point as shown in *Fig. 14*. The reduction of axial capacity is contributed by degradation of material strength, cracks in the concrete, spill and damage of the concrete and buckling of the longitudinal bars. The FE model fails to simulate the situation where concrete are smashed and falls from the column. However, the

inaccuracy after peak point, the calculated results present a good reference of the capacity of the column.

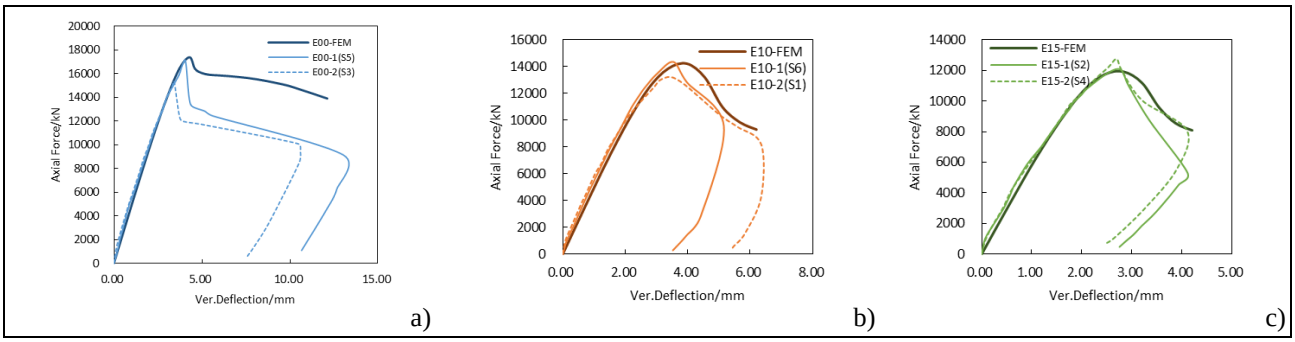

Fig.14. Phase 1: Axial force vs. vertical deflection.

A new extended method has been developed in order to design the composite columns with several steel profiles embedded. The method is an extension of the Plastic Distribution Method and takes into account all the assumptions that are defined in EC 4 - Clause 6.7, see [4]. Comparing the adapted simplified method and FEM models, similar results to the experimental part are obtained, as shown in *Fig. 15*. The simple method can be kept to make and easily "hand-made" evaluation of the axial force-bending moment interaction curve

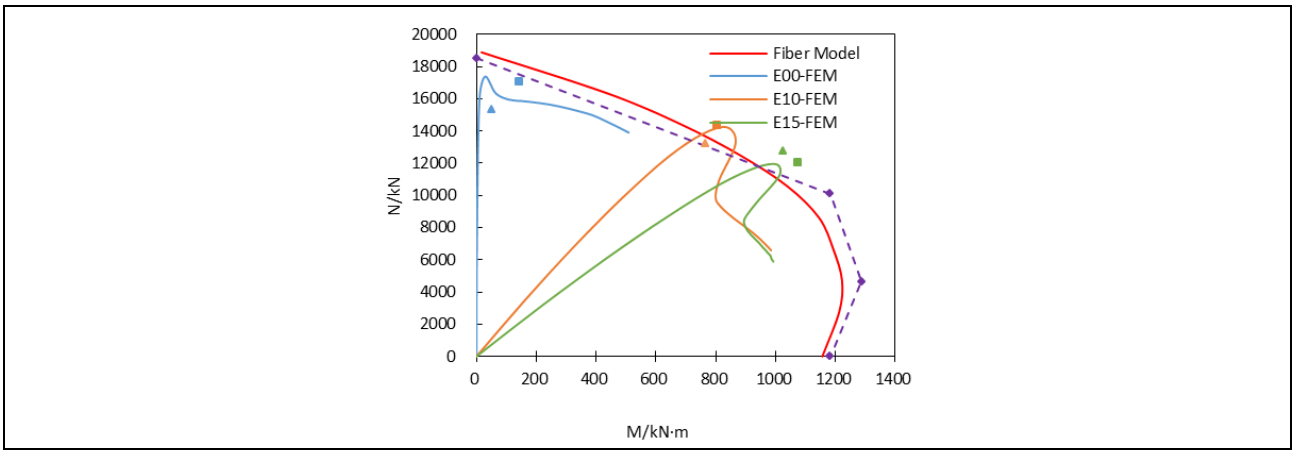

Fig.15. Phase 1: Interaction curve bending moment - axial force constructed using FEM models.

Additional deformation and stress distribution findings based on FEM results are detected. Deformations correspond to the experimental data for both purely axial and eccentric specimens.
The calculated axial capacity is presented in *Table 4*. It can be observed that numerical results correspond to experimental values.

Table 4. Phase 1: Axial force capacity – comparisons

Specimen ID	Calculated capacity /kN	Experimental capacity /kN	Ratio of calculated capacity to experimental capacity
E00-1	17392	17082	1.018
E00-2		15325	1.135
E10-1	14227	14360	0.991
E10-2		13231	1.075
E15-1	11924	12041	0.990
E15-2		12759	0.935

4 CONCLUSIONS

Two series of experimental sets were conducted to validate the performance and behaviour of mega columns with several embedded steel profiles. The two phases result in accordance with the expected results. The specimens fail in combined compression and flexure patterns.
The full composite action can be determined during the test, even though the steel sections are not connected to one another. Test results of this test program reveal that the 'Plane Section Assumption' is generally valid for specimens with an e/h=10% and an e/h=15%, but the interface slip grew with the eccentricity, which suggests that the shear demand is relatively larger for mega columns.
The ductility in terms of 'moment vs. curvature' of the static specimens is excellent. Deformation capacities of quasi-static specimens meet the minimum requirement specified by the codes. The energy consumption of the specimens is reliable, indicating a good seismic performance.
The code provisions allow the use of reduced stiffness of a concrete member, or composite member, to calculate the first order elastic reaction of the structure. This is a simplified way to account for the second order effect and concrete crack under medium or severe earthquakes. Test results of this program support the conclusion that the stiffness reduction factor can be taken 0.6 based on the EC4 method (the factor is applied to the concrete part only).
The concrete core, surrounded by the steel profiles, is highly confined, thus increasing the ductility of the composite column.
Both the static and quasi-static specimens show sufficient deformation capacity. In static tests, the specimens are able to maintain the bending moment at the maximum requirement, while the curvature is developed until column failure. In quasi-static tests, the ultimate drift ratios of the specimens meet the minimum requirement specified by the technical specification for concrete structures of tall building in Chinese code (JGJ 3 - 2010) [6].
As previously stated, no available design standards provides information on how to properly design reinforced column sections with more than one embedded steel profile. A detailed report has been prepared which contains a simplified method for evaluation of flexural capacity based on the plastic stress distribution, see [4]. The method has been validated using the experimental campaign presented in this paper.
Mega column section layout has been provided by MKA based on actual project requirements for high-rise buildings within China today.

5 SUMMARY AND ACKNOWLEDGMENT

This project was coordinated by the Council of Tall Buildings and Urban Habitat (CTBUH). The structural engineering firm Magnusson Klemencic Associates (MKA) provided background studies on composite mega columns projects. The China Academy of Building Research (CABR) was engaged to develop the testing program for the subject columns. The authors gratefully acknowledge the support and contributions from these organizations.

REFERENCES

[1] EN 1994-1-1, "Design of composite and concrete structures", 2004.

[2] Deng Fei et all, "Performance and capacity of isolated reinforced concrete columns and design approaches", CABR testing report, Beijing, China

[3] JC. Gerardy et al., Composite mega columns: testing multiple, concrete-encased, hot rolled steel sections, CTBUH publication, 2016.

[4] Plumier et all. "Design of columns with several encased steel profiles for combined compression and bending". Final report created for ArcelorMittal website, 2012

[5] JC. Gerardy et al., Composite mega columns: testing multiple, concrete-encased, hot rolled steel sections, CTBUH publication, 2016.

[6] JGJ 138-2016, "Code for design of composite structures", 2016.